

The torsional behavior of reinforced self-compacting concrete beams

Abdulkadir C. Aydın* and Barış Bayrak

Department of Civil Engineering, Faculty of Engineering, Ataturk University, 25240, Erzurum, Turkey

(Received September 12, 2018, Revised May 18, 2019, Accepted June 4, 2019)

Abstract. Torsional behaviors of beams are investigated for the web reinforcement and the concrete type. Eight beams with self-compacting concrete (SCC) and twelve beams with conventional concrete (CC) were manufactured and tested. All the models manufactured as the 250×300×1500 mm were tested according to relevant standards. Two concrete types, CC and SCC were designed for 20 and 40 MPa compressive strength. From the point of web reinforcement, the web spacing was chosen as 80 and 100 mm. The rotation angles of the concrete beams subjected to pure torsional moment as well as the cracks occurring in the beams, the ultimate and critical torsional moments were observed. Moreover, the ultimate torsional moments obtained experimentally were compared with the values evaluated theoretically according to some relevant standards and theories. The closest estimations were observed for the skew-bending theory and the Australian Standard.

Keywords: reinforced concrete; self-compacting concrete; torsion; rotation capacity; ductility

1. Introduction

Concrete is a multiphase and heterogeneous material. It's widely utilization all over the world is the result of economic and excellent versatility. However, the shear strength of cement-based composite is one of the main concerns. Specifically, the reinforcement is the key concept for that types of these advantages. To gain the related strength for shear in reinforced concrete members, web reinforcement is used. However, the evaluation of structural design concept gathers very near reinforcement (Bentur *et al.* 2001, Kılıç *et al.* 2003, Kim *et al.* 2010, Gesoğlu *et al.* 2014).

The concrete technology researches gave us the opportunity of self-compacting type special concretes. The heterogeneity of cement-based composites, non-symmetrical loading conditions, and structural plans, etc. are the main causes of torsional moments. As a global concern, the torsional behavior occurs with other axial and shear type forces in the structures. So, pure torsion is an academic subject (Patil and Sangle 2016).

In the recent years, the researchers have investigated the characteristics, and durability properties of SCC. Afterwards, the researchers have tended to the material properties of SCC (Geseoglu *et al.* 2015, Alhussainy *et al.* 2016, Kurt *et al.* 2016, Pineaud *et al.* 2016). The conventional works of SCC have handled to subject to the SCC without reinforcement, as a special concrete. However, the reinforced concrete properties of SCC have been investigated, in this study.

In the previous study about torsional behavior (Bernardo and Lopes 2013, Yang *et al.* 2013, Deifalla and Ghobarah

2014, Lopes and Bernardo 2014, Behera *et al.* 2016), the researchers mostly have investigated the torsional behavior of beams with conventional concrete (CC). In this paper, the torsional behavior of the reinforced concrete (RC) beams that were manufactured with SCC and CC have been investigated, and compared with each other.

This paper reports the results of an experimental program, which aimed to gain a better understanding of the torsional behavior of RC beams with SCC and CC under pure torsion. The work presented here is a comparison to the torsional behavior of reinforced SCC and CC beams. Furthermore, the reinforced beams with CC and SCC also were investigated to the cracks occurred due to torsional moment, possibility using of standards, American Concrete Institute (ACI-318), Eurocode-2, Turkish Standard (TS500), Australian Standard (AS), British Standard (BS) and empirical formulas about ultimate torsional moment. The torsional moment values achieved according to the theories, namely plastic and skew-bending theories were compared to the experimental results. Moreover, the critical torsional moment, the relationship between torsional moment capacity and rotation angles were examined, throughout this work.

1.1 Self-compacting concrete

The SCC is the concrete that flows itself and fills the formwork without vibration (Khayat 199). Segregation resistance and the ability of SCC to remain homogenous and stable are necessary (EFNARC 2002). The fluidity and viscosity of SCC are stabilized by water/powder ratio, superplasticizer, and a viscosity modifying admixture. These properties of SCC are provided fine filling ability, passing ability, etc. (Aydın 2007, Türkmen *et al.* 2010, Djelloul *et al.* 2018, Maali *et al.* 2019).

A lot of researchers have tended to SCC for its ability to compact without vibration. Ever since two decades, several

*Corresponding author, Professor
E-mail: acaydin@atauni.edu.tr

Table 1 The formulas of ultimate and critical torsional moment

The formula	The formulas about critical/ultimate torsional moment
Elastic Theory (Csikos and Hegedus 1998)	$T_e = \alpha_e x^2 y f_{ctk}$ (1)
Plastic Theory (Csikos and Hegedus 1998)	$T_p = \alpha_p x^2 y f_{ctk}$ (2)
	$\alpha_p = \left(\frac{1}{2} - \frac{1}{6} \frac{x}{y}\right)$ (3)
Skew-Bending Theory (Csikos and Hegedus 1998)	$T_{sb} = \frac{x^2 y}{3} f_{cts}$ (4)
ACI318	$T_{ACI} = f_{ys} (A_{sw}/s) 2A_o \cot\theta$ (5)
Eurocode-2	$T_{EU} = 2A_k \sqrt{\frac{A_{sw} f_{ywd}}{s}} \sqrt{\frac{A_{sl} f_{yld}}{u_k}}$ (6)
Turkish Standard (TS500)	$T_{TS} = \frac{A_{sw} 2A_k f_{ywd}}{s}$ (7)
Australian Standard (AS3600)	$T_{AS} = f_{ys} \left(\frac{A_{sw}}{s}\right) 2A_t \cot\theta$ (8)
British Standard (EN2004)	$T_{BS} = \frac{A_{sv} 0.8x_1 y_1 (0.87f_{ys})}{s}$ (9)
The ultimate torsional moment by Hsu (Avanish and Parekar 2010)	$T_u = 0.13b^2 h \sqrt{f_{cu}}$ (10)
The ultimate torsional moment by Rauch	$T_u = T_c + KA_s A_s^1 \left(\frac{f_{ys}}{s}\right)$ (11)
Thin-Walled Tube Theory for critical torsional moment (Valipour and Foster 2010)	$T_{cr} = [1 + (n - 1)\rho] \left(\frac{A_c^2}{u_c}\right) f_{cr}$ (12)
Turkish Standard for critical torsional moment (TS500)	$T_{TS} = 1.35 f_{ctd} S$ (13)
The critical torsional moment by Hsu (Avanish and Parekar 2010)	$T_{cr} = \frac{1.015}{\sqrt{b}} b^2 h \sqrt{f_c} + \left(0.66m \frac{f_{yd}}{f_{ywd}} + 0.33 \frac{h_j}{b_j}\right) \frac{A_{sw} f_{ywd} h_j b_j}{s}$ (14)
	$m = \frac{A_s s}{2(h_j + b_j) A_{sw}}$ (15)
The critical torsional moment by Kuyt (1968)	for web $T_{cr} = A_{sw} f_{ywd} \frac{2A_c}{s} \cot\theta$ (16)
	for longitudinal reinforcement $T_{cr} = \frac{2A_k A_{sl} f_y}{u_k} \text{tg}\theta$ (17)
The critical torsional moment by Lampert and Thurliman (1968)	for web $T_{cr} = \frac{2A_k A_{sw} f_{ywd}}{s} \text{ctg}\theta$ (18)
	for longitudinal reinforcement $T_{cr} = \frac{2A_k A_{sl} f_y}{u_k} \text{tg}\theta$ (19)

researchers have been conducted on SCC (Aydın *et al.* 2010, Verna and Misra 2015). SCC emerged in the late 80s in Japan (Djelloul *et al.* 2018). SCC was developed at the University of Tokyo in 1986 by Prof. Okamura and his team. A few of best features are that it can be compacted purely by means of their own weight without the need of vibration (Pineaud *et al.* 2016). SCC is an innovative concrete characterized by its ability to flow under its own weight without segregation or blocking (Gesoglu *et al.* 2012, Naik and Vyawahare 2013, Sadek *et al.* 2016). Therefore, SCC can be used without segregation where it is the difficult to cast such as underwater concreting, beam column joints (Okrajnov and Vasovic 2009, Naik and Vyawahare 2013, Sadek *et al.* 2016). Because of the advantages of SCC, SCC has gained acceptance by the construction industry (Golafshani and Ashour 2016, Salhi *et al.* 2017). When the SCC is compared with CC, the reduction of construction time, labor, equipment, low noise on the ground of the elimination of vibrating equipment and hard to reach areas easier are the advantages of SCC (Nehdi *et al.* 2004, Okrajnov and Vasovic 2009, Sadek *et al.* 2016).

Because of these advantages of SCC, SCC was used to the important building all over the world such as Burj Khalifa at Dubai, National Museum of 21st. Century Arts at Italy, Dragon Bridge at Spain, etc. (Okrajnov and Vasovic 2009, Deeb 2013, El-Attar *et al.* 2016).

SCC has similar components such as CC. However, the low water/cement ratio, increasing paste volume, superplasticizer, limiting aggregate content, mineral additives such as limestone, fly ash, silica fume are different from CC mixes. In this study, silica fume was used as mineral additive in the preparation of SCC mixes. Although the SCC mixes are similar to the CC mixes, the fresh and hardened properties of SCC are different from the CC ones.

Apart from this work, the previous studies (Gesoglu *et al.* 2014, Aydın *et al.* 2015a, Kurt *et al.* 2016a, Kurt *et al.* 2016b, Pineaud *et al.* 2016) are investigated some mechanical properties, etc., of SCC without reinforcement. The key point of this work is to investigate the influence of SCC characteristics, but not the compressive strength, to the torsional behavior of reinforced concrete beams.

1.2 Torsional moment

Torsion is the cross-section rotation of the elements on the same axis under the effect of torsional moments. In the structures, torsional moment occurs at the longitudinal axis of element, specifically when the force acts eccentrically. However, this torsional moment is not very important for the ultimate limit state. Torsional moment does not occur alone in the structures. The bending moment and shearing force occur with torsional moment. Thus, the pure torsional moment is the theoretical case (Kaminski and Pawlak 2011, Chalioris and Karayannis 2013). The pioneer studies about torsion of RC beams were published in the beginning of the last century.

In this study, plastic, skew-bending (Csikos and Hegedus 1998) theories; Turkish Standard (TS 500), the formula of Hsu (1968), the formula of Kuyt (1968), the formula of Lampert and Thurlimann (1968), thin-walled tube theory (Valipour and Foster 2010) for critical torsional moment and ACI318, Eurocode-2, Turkish Standard (TS500), Australian Standard (AS2001), British Standard (EN 2004), the formula of Hsu (Avanish and Parekar 2010), and the formula of Rauch for ultimate torsional moment was used to calculate the torsional moment. The related formulas for ultimate and critical torsional moment are given in Table 1.

In the elastic theory (Csikos and Hegedus 1998), the largest shear stresses occur at the mid-point of the long edge. Since the behavior of concrete is either not exactly elastic or plastic, the elastic theory gives results over the torsion capacity. The plastic theory gives results less than the torsion capacity. According to the elastic theory, the largest shear stress in the cross section occurs at the mid-point of the long edge. The plastic theory (Csikos and Hegedus 1998) assumes that, the entire sections show plastic behavior; and the shear stress is the same at each point of the section. According to the plastic theory, the plastic beam behavior at the moment of collapse is occurring without torsion, while the section is not entirely plastic. The first crack in the concrete element starts with a 45-degree angle on one of the big side surfaces of the beam for the skew-bending theory (Csikos and Hegedus 1998). Then, the cracks extend diagonally to the lower and upper surfaces, and the concrete element on the plane connecting the existing crack ends on all the surfaces. Rauch assumed that both steel and concrete are elastic. The lateral reinforcement is to take the full amount of the principal tension, and all the reinforcements in the section reach their yield stresses, while the K constant was as $2\sqrt{2}$ in the equation of Rauch.

Hsu (Avanish and Parekar 2010) suggested the equation 10, based on the skew-bending theory to obtain the ultimate torsional moment for rectangular RC beams, on the basis of his experience.

2. Experimental

2.1 Experiments

The experimental setup of the torsional RC and self-

Table 2 Chemical and physical properties of cement

Chemical properties cement composition							
SiO ₂	Al ₂ O ₃	Fe ₂ O ₃	CaO	MgO	SO ₃	Na ₂ O	K ₂ O
18.11	4.60	2.96	64.49	2.34	2.95	0.13	0.66
Physical properties							
Specific Gravity (g/cm ³)	Specific Surface (cm ² /g)	Setting time (min)					
		initial	final				
3.15	3954	140	280				

compacting reinforced concrete (SCRC) beams is presented in Fig. 1 (Maali *et al.* 2015, Maali *et al.* 2016, Maali *et al.* 2017, Maali *et al.* 2018). The RC and SCRC beams are compared with each other by neglecting the frictional forces between the models and the setup. Two steel plates in the form of hollow boxes with a depth of 300 mm were used for both the right and left ends of the beams. As a rigid loading apparatus, 1460 mm HEB160 type steel profile was used in the experiments.

The vertical load was applied to the central of HEB160 profile. The six linear variable differential transformers (LVDTs) were used to measure the deflection and to calculate the rotation of the cross-section of the beams. The vertical load was applied until beam failure, and the critical torsional moments (T_{cr}), the cracking torque of beams, ultimate torsional moments (T_u), the maximum torque of the specimens was recorded. Furthermore, the angle of rotation at initial cracking, θ_{cr} , θ_u , and the angle of rotation at maximum torque were observed.

In this study the specimens were divided into 8 groups: CC was 20 MPa with 80 mm web spacing (WS), CC was 20 MPa with 100 mm WS, CC was 40 MPa with 80 mm WS, CC was 40 MPa with 100 mm, SCC was 20 MPa with 80 mm WS, SCC was 20 MPa with 100 mm WS, SCC was 40 MPa with 80 mm WS, and SCC was 40 MPa with 100 mm. Furthermore, the SCC mixtures were prepared with the fine aggregates (0-5 mm) and coarse aggregates (5-15 mm), ordinary Portland cement (CEM I 42.5 R) conforming to the TS EN 197-1, silica fume, and superplasticizer. The chemical and physical properties of cement CEM I 42.5R are shown in Table 2.

The developments in construction and concrete technology have provided dense reinforcement details in RC members and SCC technology, which is easy to settle in narrow zones. However, there is no study evaluating these two technologies together, according to authors' point of view. Therefore, torsional behaviors of highly reinforced SCRC and CC beams are investigated throughout this study. The objective of this study is to examine the effect of concrete type and strength class on the torsional behavior of RC and SCRC beams, including WS affect for the RC and SCRC beams.

The load was applied to the beams through a 900 kN capacity hydraulic pump. The all beam models were placed in all-purpose hydraulic pump, and the load was increased until the failure of the beam. The load was increased gradual rate and was recorded through a data logger. The vertical deflections of the beams are measured at six different points using linear variable displacement transducer (LVDT). The lay-out of the LVDTs are

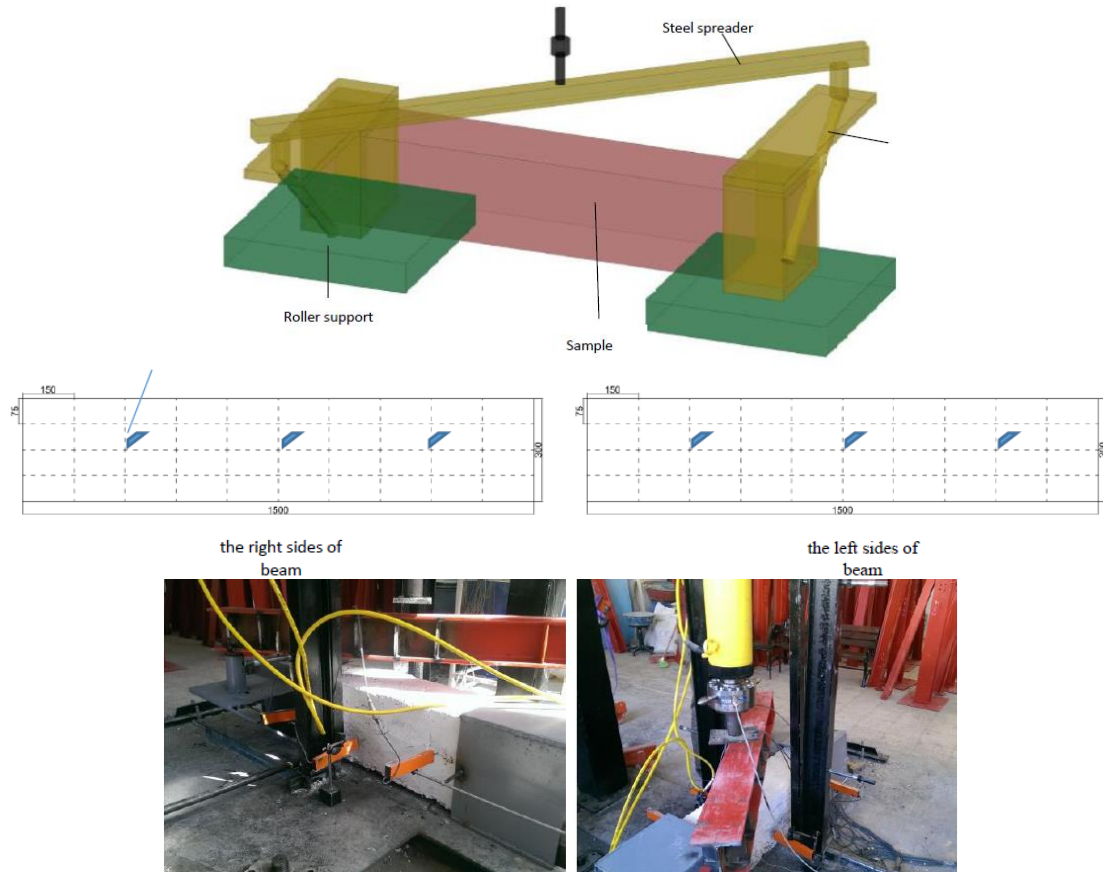


Fig. 1 Test setup and detail of the HEB160 profile

illustrated in Fig. 1.

The mixtures were prepared in a laboratory mixer at Ataturk University, Structure & Construction Materials Laboratory of Engineering Faculty. The mix proportions for SCC and CC is given at Table 3. Firstly, fine and coarse aggregates, cement, and silica fume were mixed for about 3 minutes. Next, 1/3 of total water was added slowly. This was followed by the rest of water for 2 minutes. All mixing was mixed about 5 minutes. SCC mixing requires usually more mixing process time than conventional concrete mixing. The SCC was produced according to the Self-Compacting Concrete Committee of EFNARC.

The fresh concrete tests were performed to determine the rheological properties of the SCC. The flow rate of SCC depends on the viscosity of the concrete. The ability and workability of SCC can be determined by filling ability, resistance to segregation and passing ability (EFNARC). At the fresh state of SCC mixes, three types of workability tests, namely slump flow, *L*-box, *V*-funnel, were examined according to the procedure recommended by EFNARC committee. Slump flow test is to examine filling ability of SCC without any obstruction. The feature of *L*-box is to determine the passing ability of SCC. The aim of *V*-funnel test is to determine the viscosity of SCC. Test results that are about *L*-box, *V*-funnel and slump flow tests are presented in Table 4 for C20 and C40. The illustration of slump flow test for SCC specimens is shown in Fig. 2. For each beam, three cubes (150 mm×150 mm×150 mm) were casted as control specimens. Cubes were tested for

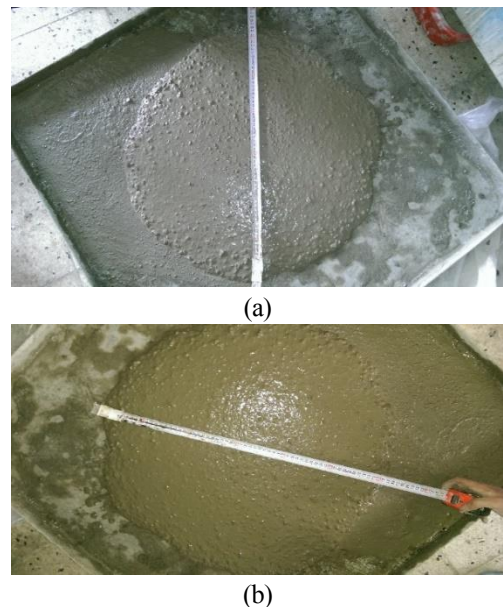


Fig. 2 The slump flow test result for (a) C20 with SCC specimens (b) C40 with SCC specimens

compressive strength at 28 days. Moreover, each beam was cured twice a day for 27 days after framework was removed, before the test day. The target compressive strength was 20 MPa and 40 MPa for both SCC series and CC series. The characteristic compressive strength of concrete (f_{ck}) was 26.7 MPa.

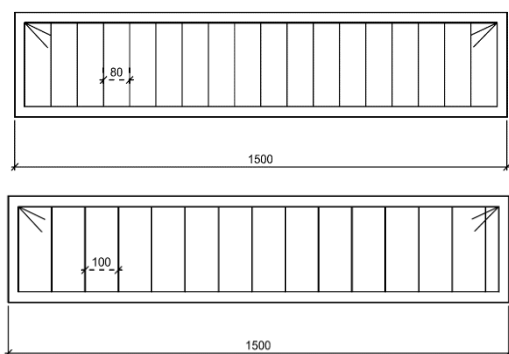


Fig. 3 The geometry and reinforcement details of the beams (all units are in millimeter)

Table 3 CC and SCC mix design

	CC		SCC	
	20 MPa	40 MPa	20 MPa	40 MPa
Characteristic cube strength	20 MPa	40 MPa	20 MPa	40 MPa
Cement	300 kg/m ³	320 kg/m ³	300 kg/m ³	324 kg/m ³
Coarse aggregate*	749 kg/m ³	780 kg/m ³	679 kg/m ³	691 kg/m ³
Fine aggregate	1010 kg/m ³	1225 kg/m ³	1102 kg/m ³	1121 kg/m ³
Water/binder ratio	0.64	0.50	0.64	0.47
Silica fume	-	-	23 kg/m ³	26 kg/m ³
Superplasticizer	-	-	6 kg/m ³	7 kg/m ³
Density of superplasticizer	1.19±0.01 g/cm ³			
pH of superplasticizer	9.5±1.0			
Chloride content of superplasticizer	< 0.10 M			
Alkali content of superplasticizer	< 0.10 M			

* The maximum aggregate size for CC and SCC was 32 mm and 16 mm, respectively

2.2 The beam details

The experimental program reported in this research included twenty (20) RC and SCRC beams with rectangular cross-section subjected to pure torsion. The twelve (12) RC specimens consisted of CC, whereas the eight (8) specimens consisted of SCC that were the 250×300 mm in cross-section and 1500 mm in length were used to determine the torsional behavior. According to the Turkish Standard, minimum cross-section for beams is 250×300 mm and so cross-section of the beams was selected 250×300 mm. The beam length and web spacing were chosen to be 1500 mm in order to be suitable for the studies in the literature. The 12 of the beams were manufactured with CC and 8 of specimens were manufactured with SCC. Fig. 3 shows the geometry, the cross sectional and reinforcement details of tested beams. The diameters of the reinforcements were 16 and 8 mm for longitudinal and web reinforcement, respectively.

The longitudinal reinforcement ratio is 0,008 and the yield strength of both longitudinal reinforcement and transversal was 420 MPa. The dimensions of the beams, reinforcements were kept same for each group of all RC and

Table 4 Test on fresh concrete

Concrete Class	Slump flow D (mm)	L -box	Funnel (s)
C20	640	0.11	9.8
C40	640	0.14	8.6

Table 5 Some properties of tested beams

The name of beams	Concrete Type	Concrete Strength Class (MPa)	Web Spacing (mm)
CC_C20_SS80	CC	20	80
CC_C20_SS100	CC	20	100
CC_C40_SS80	CC	40	80
CC_C40_SS100	CC	40	100
SC_C20_SS80	SCC	20	80
SC_C20_SS100	SCC	20	100
SC_C40_SS80	SCC	40	80
SC_C40_SS100	SCC	40	100

SCRS beams. Some properties of tested beams are given in Table 5. The transversal and longitudinal reinforcements were designed according to the Turkish and ACI Standards. The longitudinal and transversal reinforcement of the tested beams were chosen as respectively 16 and 8 mm diameters for their common usage according to relevant literature. Besides, web spacing was decided as 80 and 100 mm to observe the effect of transversal reinforcement ratio of RC and SCRC beams. Furthermore, the concrete cover was 30 mm for all samples.

3. Results and discussion

3.1 Cracking pattern and failure mode

The failures of the models were the abrupt type, and after the exceeding critical torsional moment. The first cracks appeared on the top side of the tested beams. The cracks were formed at an angle of about 45 degrees with the horizontal axis of the beam. As a result of the shear stress does not occur or is about zero when the tensile force affects the shear plane in parallel or perpendicularly, the shear stress reaches its maximum value. The first crack that occurred on the beams was observed on the lateral surface of tested beams.

The gradation of the SCC resulted narrower crack widths, owing to the maximum aggregate size was 32 mm for CC and 16 mm for SCC. Decreasing maximum aggregate size affects the distance between grains inside of the concrete, and the crack formation occurs through the interface between paste and the aggregate, where the lowest strength occurred. Crack width increased by loading, after the first crack appeared. The first crack width was the greatest for all models. The cracks' widths, which are average of readings at same location for every group of models are given in Table 6. The crack widths were measured basically with a crack ruler. Table 6 presents the crack widths in SCC series were the crack widths are 70% narrower than the CC ones. Moreover, increasing the concrete strength class decreased the crack width in both

Table 6 Maximum crack width of tested beams

Model	Crack width (mm)	Model	Crack width (mm)	Crack width decrease (%)
CC20SS80	2.7	SCC20SS80	2.5	8.42
CC20SS100	6.9	SCC20SS100	3.3	52.17
CC40SS80	4.6	SCC40SS80	1.4	69.57
CC40SS100	3.4	SCC40SS100	2.0	41.17



Fig. 4 The first second and third cracks in the tested beam

CC and SCC series. Similarly, reducing the web spacing decreased the crack width in both CC and SCC series.

The first observed crack suddenly advanced downward and diagonally. The first cracks on the tested beams appeared on parts near the braces. The starting points of the cracks occurred in the upper part of the beams and extended downwards along the side surface of the beam due to the increasing load. The other cracks followed the first crack occurred almost in the mid-point of the beam. The second and third cracks formed like branches around the first crack. In some models, the second and third cracks occurred about

10 cm away from the first crack. The branching on the RC beams were more than the branching in the SCRC beams, as a result of gradation. The first and second cracks are shown in Fig. 4. The cracks that were occurred on the beams with CC and SCC is shown Fig. 5. Based on the cracking formation of each beam, the diagonal cracks can be observed from this figure.

For these photographs, it can be observed that the RC beams showed sudden failure (Fig. 5(b)), whereas the SCRC beams also failed in a same manner, but they showed narrower crack widths than the RC ones.

Fig. 5 shows that even though the number of cracks in the CC models (RC ones) are less than SCRC beams. The maximum crack widths in RC beams are greater than SCRC ones, as a result of gradation mentioned above. Therefore, the crack patterns between the aggregate and the cement paste are closer to one another in the SCRC samples, where the lowest strength and the crack formation occurred through the interface between paste and the aggregates.

3.2 Torsion according to the standards and theories

The theoretically torsional moment values based on the standards concerning the torsional moment capacity (T_u) were compared. Furthermore, the experimental and theoretical critical torsional moment (T_{cr}), which is caused the first crack, were also compared in this section. Moreover, the rotation angles (θ_u) for the torsional moment capacity and the rotation angles (θ_{cr}) for the critical torsional moment were observed. The experimental torsional moment capacity and the critical torsional moment were compared according to ACI, EU, TS, AS3600, BS8110 standards and the empirical torsional moment capacity by Rauch and Hsu. Fig. 6 presents the comparison of

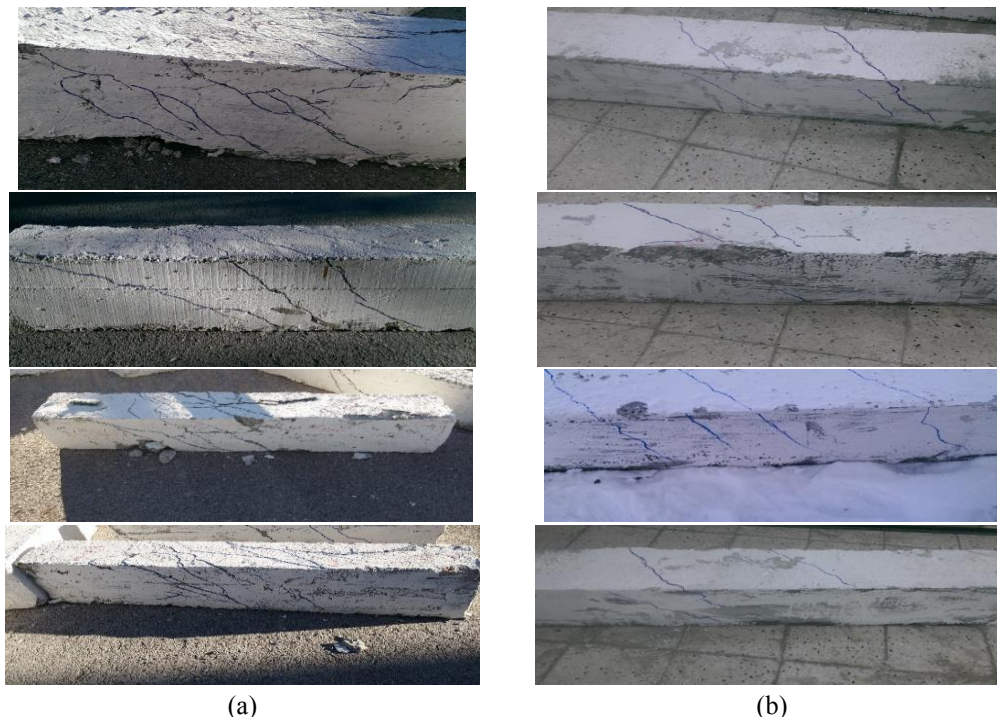


Fig. 5 (a) The cracks on RC series (b) The cracks on SCRC series

Table 7 The experimental and theoretical ultimate torsional moment and twist results

Model Name	T_u (exp*) (kNm)	θ_u (exp) (deg/m)	T_{cr} (exp) (kNm)	θ_{cr} (exp) (deg/m)	ACI (kNm)	EU-2 (kNm)	TS (kNm)	AS3600 (kNm)	BS8110 (kNm)	Hsu Formula (kNm)	Rauch Formula (kNm)
CC20SS80	11.71	3.39	10.72	3.30	9.30	6.68	10.94	12.88	7.61	11.34	23.18
CC20SS100	11.47	3.46	9.26	3.23	7.44	5.97	8.75	10.31	6.10	11.34	19.84
CC40SS80	14.07	3.46	13.88	3.18	9.30	6.68	10.94	12.88	7.61	15.16	25.62
CC40SS100	13.38	3.74	12.23	3.58	7.44	5.97	8.75	10.31	6.10	15.16	22.29
SCC20SS80	16.19	4.77	14.99	4.71	9.30	6.68	10.94	12.88	7.61	11.34	23.18
SCC20SS100	13.88	3.15	12.14	3.10	7.44	5.97	8.75	10.31	6.10	11.34	19.84
SCC40SS80	20.34	4.19	19.28	4.09	9.30	6.68	10.94	12.88	7.61	15.16	25.62
SCC40SS100	18.54	5.02	16.02	4.99	7.44	5.97	8.75	10.31	6.10	15.16	22.29

*exp: experimental

Table 8 Experimental and theoretical critical torsional moment results

Model Name	T_{cr} (exp) (kNm)	TS (kNm)	Hsu (kNm)	Thin-Walled Tube (kNm)	Kuyt (kNm)		Lampert (kNm)	
					for stirrup	for longitudinal reinforcement	for stirrup	for longitudinal reinforcement
CC20SS80	10.72	8.77	12.51	8.16	18.00	1.18	10.95	4.1
CC20SS100	9.26	8.77	11.08	8.16	14.4	1.05	8.76	4.1
CC40SS80	13.88	12.49	14.74	11.12	18.00	1.18	10.95	4.1
CC40SS100	12.23	12.49	13.32	11.12	14.4	1.05	8.76	4.1
SCC20SS80	16.58	8.77	12.51	8.16	18.00	1.18	10.95	4.1
SCC20SS100	14.99	8.77	11.08	8.16	14.4	1.05	8.76	4.1
SCC40SS80	12.14	12.49	14.74	11.12	18.00	1.18	10.95	4.1
SCC40SS100	16.02	12.49	13.32	11.12	14.4	1.05	8.76	4.1

exp: Average experimental values

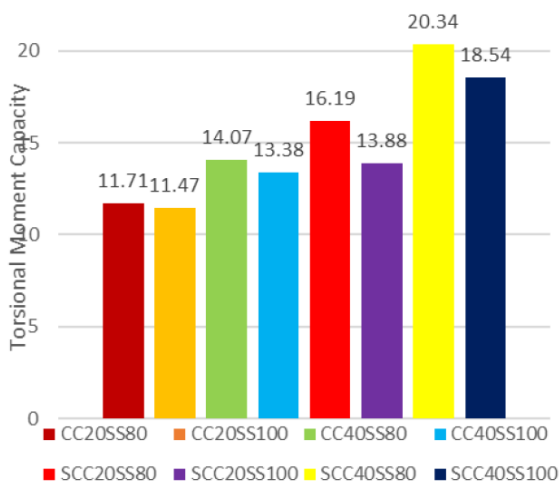


Fig. 6 The average ultimate torsional moment results of tested beams

experimental torsional moment values, also. The mentioned values in Fig. 6 are average values of three RC beams and two SCRC beams.

The experimental and theoretical results are shown in Table 7. Table 7 and Fig. 6 shows that the maximum torsional moment capacity was observed as 20.34 kNm for the SCC40SS80 beam and the minimum ultimate torsional moment as 10.67 kNm for the SCC20SS100 beam. The Eqs. (5)-(6)-(7)-(8)-(9)-(10)-(11) were used to calculate to the ACI, EU-2, TS, AS3600, BS8110, Hsu's formula and Rauch's formula, respectively. It was determined that the

low web spacing and high concrete strength class have a positive effect on the both ultimate and critical torsional moments. It was observed that there is a direct relationship between the torsional moment capacity and the rotation angle. Furthermore, Table 7 shows that the torsional moment capacity is very close to the critical torsional moment. Similarly, the rotation angle corresponding to the torsional moment capacity and the critical rotation angle are approximately the same. As a result of brittle behavior, the torsional moment capacity and critical torsional values are very similar.

Comparison of the experimental results with the theoretical ones based on the standards, the closest results were obtained for the AS. The theoretical torsional moments calculated based on the relevant standards in this study were different than each other. The reason for this is that each standard uses different approaches to calculate the sectional areas of the beams. The results that were farthest from the experimental results were the theoretical values calculated with the formula suggested by Rauch to calculate torsional moment capacity.

Another parameter evaluated in this study was the comparison of the experimentally measured critical torsional moment values with the relevant standards, and the theoretical results obtained by empirical equations. The Eqs. (12)-(13)-(14)-(16)-(17)-(18)-(19) were used to calculate to the Thin-Walled Theory, TS, Hsu's formula, Kuty's formulas, Lampert's formulas, respectively. The results of experimental and theoretical critical torsional moment values are given in Table 8. The maximum ultimate

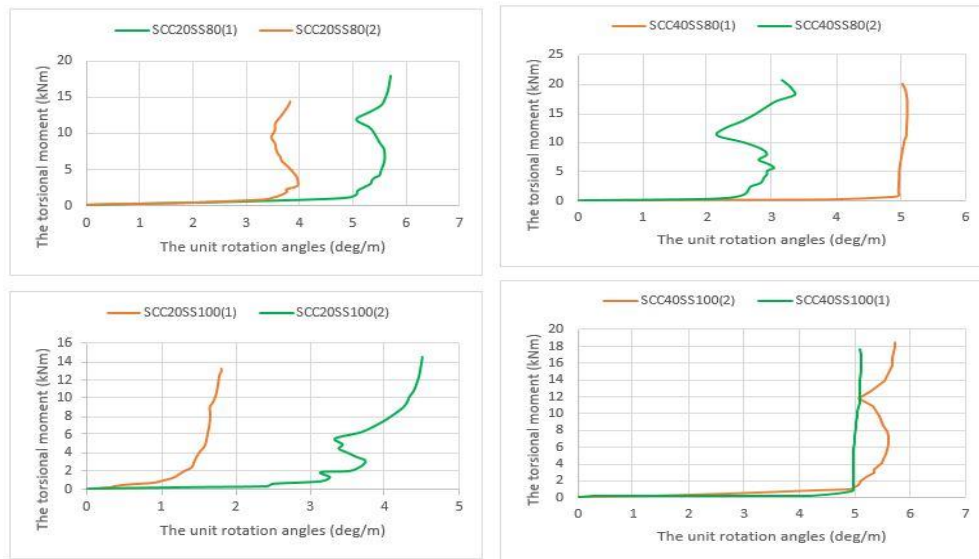


Fig. 7 The relationship between ultimate torsional moment and unit rotation angles for SCC series

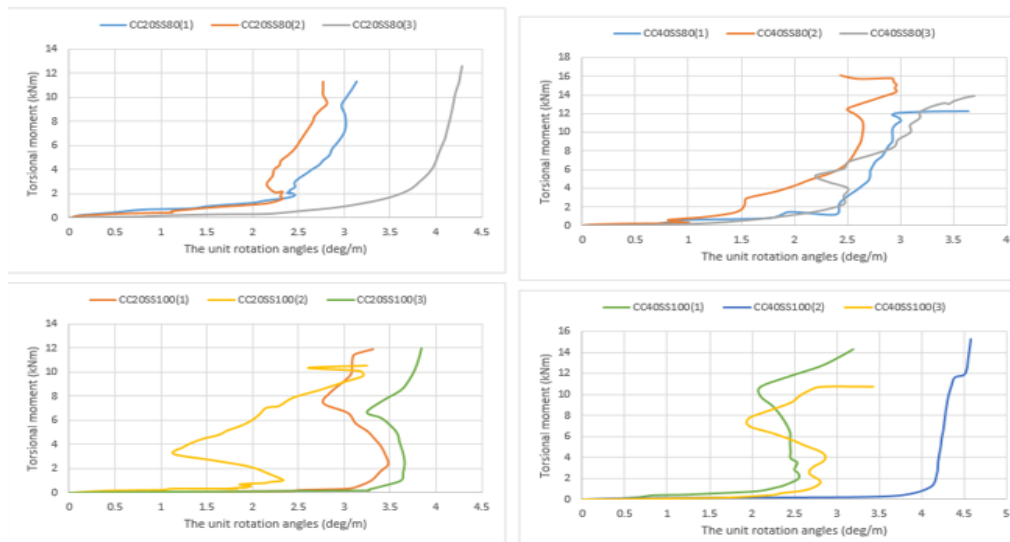


Fig. 8 The relationship between ultimate torsional moment and unit rotation angles for CC series

Table 9 Ultimate torsional moment and theories

Model Name	Experimental Ultimate Torsional Moment (kNm)	Plastic Theory (kNm)	Skew-Bending Theory (kNm)
CC20SS80	11.71	10.83	12.50
CC20SS100	11.47	10.83	12.50
CC40SS80	14.07	14.89	17.20
CC40SS100	13.38	14.89	17.20
SCC20SS80	16.19	10.83	12.50
SCC20SS100	13.88	10.83	12.50
SCC40SS80	20.34	14.89	17.20
SCC40SS100	18.54	14.89	17.20

torsional moment was 19.52 kNm for the SCC40SS80 beam. Table 8 suggests that higher concrete strength class and low web ratios have a positive impact on the critical torsional moment. The closest values to the experimental results were obtained by the formula suggested by Hsu for

the critical torsional moment. Moreover, Table 8 shows the experimental values were very close to the values calculated according to the formulas established by Kuyt and Lampert based on the stirrup in the beam section. But the values calculated according to the formulas which have been constituted by Kuyt and Lampert on the basis of longitudinal reinforcement and experimental results turned out quite different from each other.

When the average torsional moment capacities of CC40SS80 and SCC40SS80 beams are compared, it is seen that the SCRC series has a greater torsional capacity of more than 41%. Since the SCC concrete mix, has better adherence between cement paste and aggregates than CC ones. For this reason, crack formation from this interface is more difficult in SCC samples. However, the CC and SCC samples compressive strengths are similar; the gradation of SCC (maximum grain size) is less than the CC ones. Thus, the shear crack pattern elongates by the aggregate surface increase within the usage of SCC gradation. Thus, the SCC

specimens has greater torsional capacity in CC specimens (Aydin *et al.* 2007). Thus, it was experimentally observed that web had more effect on the torsional characteristics of the beams than longitudinal reinforcements. The torsional moment values, experimentally obtained, were compared with the theoretical ones, calculated according to plastic and lateral bending theories and results are given in Table 9.

3.3 Relationship between torsion and unit angles rotation

This section examines the relation of the experimentally measured torsional moment capacity to the rotational angle. The moment behavior of beams has been investigated such as the other studies (Aydin *et al.* 2015a, b). The rotation of the beams was measured using six LVDTs placed to the right and left sides of beam models.

The graphics of ultimate torsional moment-unit rotation angles for SCRC series are presented in Fig. 7. The graphics of ultimate torsional moment-unit rotation angles for RC series are shown in Fig. 8. It can be observed from the Figs. 7-8 that the ultimate torsional moments of the RC and SCRC beams demonstrate that the transverse reinforcement and concrete strength class effects the torsional capacity, ductility, as it is expected. Furthermore, it can be observed from Fig. 8 that the ductility values of the RC beams increased with the web ratio increase. As well as strength, the other desired important characteristic of a reinforced beam exposed to torsion is the ductile behavior. Ductility is an important parameter for the failure of the structures (Gunasekaran *et al.* 2016). The ductility of a beam that supposed to the torsion is the 90% of ultimate torque (Punmia *et al.* 2007). Which is implied by ductile behavior is that a beam isn't failed sudden in a brittle manner. The experiments performed so far have proved that ductile behavior is a function of shear reinforcement. When the experimental graphs are examined, the areas covered under the graphs of angle of rotation of torsional moment for SCRC series are greater than the RC ones. In other words, the failure occurred in SCRC beams were experienced in a more brittle manner than that of RC ones.

The graphics contained in the same series were virtually the same. SCRC series exhibited more brittle than the RC series. SCRC models had a larger torsional moment than the RC ones, and the torsional moment that caused the first crack reached greater values in the SCRC models.

From the test results presented in Figs. 7-8 and Tables 7-8, it is verified that the beams were manufactured with SCC exhibited substantially improved torsional performance with respect to the corresponding beams were manufactured with CC at the same web ratio. On the contrary, the beams with CC show considerably reduced torsional capacities.

There is some rotational decrease while the moment increasing, due to the crushing of the concrete at the corners of the beams' heads. Furthermore, the energy needed to form a crack, is greater than the energy needed to propagate a crack. Thus, the unit rotation angles decreased suddenly while increasing torsional moment when some graphics are inspected.

4. Conclusions

In this study, the behavior of RC beams under pure torsion was investigated. The variables are concrete type, concrete strength class, and web spacing. Each beam was analyzed under increasing pure torsion up to failure. The following conclusions were drawn:

- The torsional moment capacities of the beam specimens pertaining to a concrete strength class with greater strength, ranged up to greater values. In this context, it was experimentally determined that the torsional moment capacities of SCRC series ranged to greater values as compared to RC ones. It can be deduced that the SCC gradation characteristics has a positive impact for the reinforced concrete technology. The aggregate surface increase within the usage of SCC gradation, the shear crack pattern elongates. Thus, the torsional capacity of SCRC samples are greater than the CC ones.
- The low web spacing increased the ultimate torsional moment for all models. Furthermore, for the concrete strength classes, the torsional moment capacity increased with decreasing web spacing about 16.74% and 9.71% for the SCC20 and SCC40 group of models, respectively. Similarly, the torsional moment capacity increased with decreasing web spacing about 2.10% and 5.16% for the CC20 and CC40 group of models, respectively.
- The comparison of the experimental results with the theoretical ones based on the standards, the closest results were obtained for the AS. The torsional moment is 25.6%, 74%, 142.3%, 47.9%, and 112.74% greater than AS, ACI, EU, TS, and BS for the SCC20SS80 model, respectively. For the SCC20SS100 model, the torsional moment is 34.62%, 86.55%, 132.50%, 58.62%, and 127.54% greater than AS, ACI, EU, TS, and BS ones. Similarly, the torsional moment of SCC40SS80 model is 57.91%, 118.70%, 204.5%, 85.92%, and 167.28% greater than AS, ACI, EU, TS, and BS, respectively. Moreover, the torsional moment of SCC40SS100 model is 79.82%, 149.19%, 210.55%, 111.88%, and 203.93% greater than AS, ACI, EU, TS, and BS ones, respectively. The effect of effective cross-section area, web reinforcement, and longitudinal reinforcement on the torsional moment is familiar and intended to use within the formulations of many standards. However, the separate effect of effective cross-section area, web reinforcement, and longitudinal reinforcement on the torsional moment is greater than completely together. Thus, above-mentioned standards and relevant works have to be red-designed /re-evaluated within this scope.
- The torsional moment of CC group of models is increased about 9-29.77%, 25.91-79.83%, 75.29-124.12%, 7.03-52.91%, 53.87-119.34% greater than AS, ACI, EU, TS, and BS ones, respectively. The torsional moment values measured in the CC group of models were found more approximate to the standards than the SCC ones. The torsional moment of SCC group of models is quite higher than the standards. The

theoretical torsional moment values, especially calculated according to EU, became quite low in comparison with the other torsional moment values. The torsional moment analysis is mostly including empirical values for CC samples. Thus, these empirical values have to be re-observed according to special concretes, like crack-pattern, crack-path length included, fiber effect etc.

- The strength of concrete increased the critical torsional moment about 30% for higher strength concrete class models. Furthermore, decreasing web space from 100 to 80 mm, increased the critical torsional moment about 23.56% and 14%, for the SCC20 and CC20 group of models, respectively.

- After exceeding critical torsional moment, cracks were observed immediately, for all the models. The cracks were occurred about 45-degree angles with the horizontal axis of the RC beam in compliance with skew-bending theory. For the lower strength group of models, decreasing web spacing decreased the crack width about 60% and 24% for the RC and SCRC group of models. However, the crack width decrease was about 30% for the C40 type SCRC group of models. In other words, the crack width decreased with increasing compressive strength of all the models. Furthermore, the ultimate torsional moment capacity – critical torsional moment ratio is decreased by not only increasing compressive strength, but also with the change of concrete type from CC to SCC. The decreasing ultimate torsional moment capacity – critical torsional moment ratio is the main reason of increasing brittle failure of the specimen.

- The observed torsional moment capacities were greater than the ones according to the plastic theory, and lower than the values obtained from the skew-bending theory. However, the best approximation was obtained for the skew-bending theory. The experimental torsional moments were about 12% greater than the values from plastic theory, and about 2% lower than the ones from skew-bending theory. The torsional moment capacities evaluated for the plastic theory by using the dimensions of the sample, generally; however, for the skew-bending theory, they are acquired with the dimensions and the tensile strength of the concrete, also. Thus, the skew-bending theory resulted better estimations.

- When the standards and empirical critical torsional moments are examined, the best approximation is obtained by Hsu, used the greater number of parameters including web reinforcement, also; for the calculations, and the approximation was only about 2%.

- The SCRC models exhibited more brittle behavior than RC ones. Furthermore, the SCRC models exhibited higher torsional moment than RC ones, and the torsional moment causing the first crack increased up to greater values for SCRC models.

References

ACI 318-08 (2008), Building Code Requirements for Structural Concrete and Commentary, American Concrete Institute,

- Farmington Hills, MI, USA.
- Alhussainy, F., Hasan, H.A., Rogic, S., Sheikh, M.N. and Hadi, M.N. (2016), "Direct tensile testing of self-compacting concrete", *Constr. Build. Mater.*, **112**, 903-906.
- AS3600 (2001), Australian Standard, Concrete Structures, AS3600-2001, Sydney, Australia.
- Avinash, S.P. and Parekar, R.S. (2010), "Steel fiber reinforced concrete beams under combined torsion-bending-shear", *J. Civil Eng. (IEB)*, **38**(1), 31-38.
- Aydın, A.C. (2007), "Self compactability of high volume hybrid fiber reinforced concrete", *Constr. Build. Mater.*, **21**(6), 1149-1154.
- Aydın, A.C., Arslan, A. and Gül, R. (2007), "Mesoscale simulation of cement based materials' time-dependent behavior", *Comput. Mater. Sci.*, **41**(1), 20-26.
- Aydın, A.C., Karakoç, M.B., Düzgün, O.A. and Bayraktutan, M.S. (2010), "Effect of low quality aggregates on the mechanical properties of lightweight concrete", *Scientif. Res. Essay*, **5**(10), 1133-1140.
- Aydın, A.C., Kılıç, M., Maali, M. and Sağıroğlu, M. (2015a), "Experimental assessment of the semi-rigid connections behavior with angles and stiffeners", *J. Constr. Steel Res.*, **114**, 338-348.
- Aydın, A.C., Maali, M., Kılıç, M. and Sağıroğlu, M. (2015b), "Experimental investigation of sinus beams with end-plate connections", *Thin Wall. Struct.*, **97**, 35-43.
- Aydın, A.C., Öz, A., Polat, R. and Mindivan, H. (2015c), "Effects of the different atmospheric steam curing processes on the properties of self-compacting-concrete containing microsilica", *Sadhana*, **40**(4), 1361-1371.
- Behera, G.C., Rao, T.G. and Rao, C. (2016), "Torsional behaviour of reinforced concrete beams with ferrocement U-jacketing-experimental study", *Case Stud. Constr. Mater.*, **4**, 15-31.
- Bentur, A., Igarashi, S.İ. and Kovler, K. (2001), "Prevention of autogenous shrinkage in high-strength concrete by internal curing using wet lightweight aggregates", *Cement Concrete Res.*, **31**(11), 1587-1591.
- Bernardo, L. and Lopes, S. (2013), "Plastic analysis and twist capacity of high-strength concrete hollow beams under pure torsion", *Eng. Struct.*, **49**, 190-201.
- Chalioris, C.E. and Karayannis, C.G. (2013), "Experimental investigation of RC beams with rectangular spiral reinforcement in torsion", *Eng. Struct.*, **56**, 286-297.
- Csikós, Á. and Hegedűs, I. (1998), "Torsion of reinforced concrete beams", Research Report No. H-1521, Technical University of Budapest, Department of Reinforced Concrete Structures, Budapest, Hungary.
- Deeb, R. (2013), "Flow of self-compacting concrete", Ph.D. Dissertation, Cardiff University, Cardiff.
- Deifalla, A. and Ghobarah, A. (2014), "Behavior and analysis of inverted T-shaped RC beams under shear and torsion", *Eng. Struct.*, **68**, 57-70.
- Djelloul, O.K., Menadi Wardeh, B.G. and Kenai, S. (2018), "Performance of self-compacting concrete made with coarse and fine recycled concrete aggregates and ground granulated blast-furnace slag", *Adv. Concrete Constr.*, **6**(2), 103-121.
- EFNARC (2005), The European Guidelines for Self-Compacting Concrete: Specification, Production and Use, the Self-Compacting Concrete, European Project Group.
- EN (2004), Eurocode 2: Design of Concrete Structures- Part 1-2: General Rules-Structural Fire Design, European Standards, London, UK.
- EN (2012), Cement-Part 1: Composition, Specifications and Conformity Criteria for Common Cements, Turkish Standard Institution, Ankara, Turkey.
- Gesoglu, M., Güneyisi, E., Öz, H.Ö., Taha, I. and Yasemin, M.T. (2015), "Failure characteristics of self-compacting concretes

- made with recycled aggregates”, *Constr. Build. Mater.*, **98**, 334-344.
- Gesoğlu, M., Güneyisi, E., Özturan, T., Öz, H.Ö. and Asaad, D.S. (2014), “Self-consolidating characteristics of concrete composites including rounded fine and coarse fly ash lightweight aggregates”, *Compos. Part B: Eng.*, **60**, 757-763.
- Gesoğlu, M., Güneyisi, E.M., Kocabağ, E., Bayram, V. and Mermerdaş, K. (2012), “Fresh and hardened characteristics of self-compacting concretes made with combined use of marble powder, limestone filler, and fly ash”, *Constr. Build. Mater.*, **37**, 160-170.
- Golafshani, E.M. and Ashour, A. (2016), “Prediction of self-compacting concrete elastic modulus using two symbolic regression techniques”, *Autom. Constr.*, **64**, 7-19.
- Gunasekaran, K., Chandar, P.S., Annadurai, R. and Satyanarayanan, K. (2016), “Augmentation of mechanical and bond strength of coconut shell concrete using quarry dust”, *Eur. J. Environ. Civil Eng.*, 1-12.
- Hsu, T.T. (1968), “Torsion of structural concrete-plain concrete rectangular sections”, *Spec. Publ.*, **18**, 203-238.
- Kamiński, M. and Pawlak, W. (2011), “Load capacity and stiffness of angular cross section reinforced concrete beams under torsion”, *Arch. Civil Mech. Eng.*, **11**(4), 885-903.
- Khayat, K. (1999), “Workability, testing, and performance of self-consolidating concrete”, *Mater. J.*, **96**(3), 346-353.
- Kılıç, A., Atiş, C.D., Yaşar, E. and Özcan, F. (2003), “High-strength lightweight concrete made with scoria aggregate containing mineral admixtures”, *Cement Concrete Res.*, **33**(10), 1595-1599.
- Kim, Y.J., Choi, Y.W. and Lachemi, M. (2010), “Characteristics of self-consolidating concrete using two types of lightweight coarse aggregates”, *Constr. Build. Mater.*, **24**(1), 11-16.
- Kurt, M., Gül, M.S., Gül, R., Aydın, A.C. and Kotan, T. (2016a), “The effect of pumice powder on the self-compactability of pumice aggregate lightweight concrete”, *Constr. Build. Mater.*, **103**, 36-46.
- Kurt, M., Kotan, T., Gül, M.S., Gül, R. and Aydın, A.C. (2016b), “The effect of blast furnace slag on the self-compactability of pumice aggregate lightweight concrete”, *Sadhana*, **41**(2), 253-264.
- Kuyt, B. (1968), “Ultimate torsional resistance of rectangular reinforced concrete beams”, *Concrete*, **2**(12), 522.
- Lampert, P. and Thürlimann, B. (1968), *Torsionsversuche an Stahlbetonbalken*.
- Lopes, S. and Bernardo, L. (2014), “Cracking and failure mode in HSC hollow beams under torsion”, *Constr. Build. Mater.*, **51**, 163-178.
- Maali, M., Aydın, A.C. and Sağıroğlu, M. (2015), “Investigation of innovative steel runway beam in industrial building”, *Sadhana*, **40**(7), 2239-2251.
- Maali, M., Kılıç, M. and Aydın, A.C. (2016), “Experimental model of the behaviour of bolted angles connections with stiffeners”, *Int. J. Steel Struct.*, **16**(3), 719-733.
- Maali, M., Kılıç, M. and Aydın, A.C. (2019), “Experimental behavior of bolted connections with stiffeners”, *Steel Constr. Des. Res.*, **12**(2), 105-113.
- Maali, M., Kılıç, M., Sağıroğlu, M. and Aydın, A.C. (2017), “Experimental model for predicting the semi-rigid connections’ behaviour with angles and stiffeners”, *Adv. Struct. Eng.*, **20**(6), 884-895.
- Maali, M., Sağıroğlu, M. and Solak, M.S. (2018), “Experimental behavior of screwed beam-to-column connections in cold-formed steel frames”, *Arab. J. Geosci.*, **11**(9), 205.
- Naik, M.P.P. and Vyawahare, M. (2013), “Strength and durability investigations on self-consolidated concrete with pozzolanic filler and inert filler”, *International Journal of Engineering Research and Technology*, ESRSA Publications.
- Nehdi, M., Pardhan, M. and Koshowski, S. (2004), “Durability of self-consolidating concrete incorporating high-volume replacement composite cements”, *Cement Concrete Res.*, **34**(11), 2103-2112.
- Okrajnov-Bajić, R. and Vasović, D. (2009), “Self-compacting concrete and its application in contemporary architectural practice”, *Spatium*, **20**, 28-34.
- Patil, S.P. and Sangle, K.K. (2016), “Tests of steel fibre reinforced concrete beams under predominant torsion”, *J. Build. Eng.*, **6**, 157-162.
- Pineaud, A., Pimienta, P., Rémond, S. and Carré, H. (2016), “Mechanical properties of high performance self-compacting concretes at room and high temperature”, *Constr. Build. Mater.*, **112**, 747-755.
- Punmia, B., Jain, A.K. and Jain, A. K. (2007), *Limit State Design of Reinforced Concrete*, Firewall Media.
- Rowe, R.E. (1987), Handbook to British Standard BS 8110: 1985, Structural Use of Concrete, Palladian Publications.
- Sadek, D.M., El-Attar, M.M. and Ali, H.A. (2016), “Reusing of marble and granite powders in self-compacting concrete for sustainable development”, *J. Clean. Prod.*, **121**, 19-32.
- Salhi, M., Ghrici, M., Li, A. and Bilir, T. (2017), “Effect of curing treatments on the material properties of hardened self-compacting concrete”, *Adv. Concrete Constr.*, **5**(4), 359-375.
- TS500 (2000), Requirements for Design and Construction of Reinforced Concrete Structures, Turkish Standards Institute, Ankara, Turkey.
- Türkmen, İ., Öz, A. and Aydın, A.C. (2010), “Characteristics of workability, strength, and ultrasonic pulse velocity of SCC containing zeolite and slag”, *Scientif. Res. Essay.*, **5**(15), 2055-2064.
- Valipour, H.R. and Foster, S.J. (2010), “Nonlinear reinforced concrete frame element with torsion”, *Eng. Struct.*, **32**(4), 988-1002.
- Verma, N. and Misra, A.K. (2015), “Bond characteristics of reinforced TMT bars in self compacting concrete and normal cement concrete”, *Alexandria Eng. J.*, **54**(4), 1155-1159.
- Yang, I.H., Joh, C., Lee, J.W. and Kim, B.S. (2013), “Torsional behavior of ultra-high performance concrete squared beams”, *Eng. Struct.*, **56**, 372-383.

CC

Notations

- A_o : gross area enclosed by the shear flow path
 A_c : area of cross-section concrete
 A_e : area of core enclosed by webs
 A_k : the area enclosed by the center-lines of the effective wall thickness
 A_s : area of all longitudinal bars
 A_{sl} : cross sectional area of one leg of steel
 A_{sv} : area of the two legs of web at a section
 A_{sl} : cross-sectional area of longitudinal bars
 A_{sw} : the cross-sectional area of webs
 A_t : area enclosed by the center lines of longitudinal bars
 b : horizontal length of beam
 b_j : the cross-sectional width in the axis of the webs
 f_c : cube strength of plain concrete
 f_{cu} : cube strength of plain concrete
 f_{ctd} : tension strength of concrete
 f_{ctk} : characteristic tensile strength
 f_{cts} : splitting tensile strength

- f_{cr} : denotes the cracking strength of concrete
 f_y : the yield stress of longitudinal bars
 f_{yd} : the yield stress of longitudinal bars
 f_{yld} : the yield stress of longitudinal bars
 f_{ys} : the yield stress of longitudinal bars
 f_{ywd} : the yield stress of webs
 h : vertical length of beam
 h_e : the cross-sectional height in the axis of the webs
 K : Rauch constant
 n : modular ratio
 s : the center-to-center spacing of webs
 S : strength of torsional moment
 T_{AS} : torsional moment value for Australian Standard
 T_{ACI} : torsional moment value for ACI Standard
 T_{BS} : torsional moment value for British Standard
 T_C : torque carried by concrete based on elastic theory
 T_{cr} : critical torsional moment
 T_e : torsional moment value for elastic theory
 T_{EU} : torsional moment value for Eurocode-2 Standard
 T_p : torsional moment value for plastic theory
 T_{sb} : torsional moment value for skew-bending theory
 T_{TS} : torsional moment value for Turkish Standard
 T_u : ultimate torsional moment
 u_c : perimeter of the concrete cross-section
 u_K : perimeter of the area A_k
 x : horizontal length of beam
 x_1 : center-to-center of the shorter of webs
 y : vertical length of beam
 y_1 : center-to-center of the longer of webs